
Layout-and-Retouch: A Dual-stage Framework for Improving Diversity in Personalized Image Generation

Kangyeol Kim^{1,3*}, Wooseok Seo^{2*}, Sehyun Nam², Bodam Kim²,
 Suhyeon Jeong², Wonwoo Cho^{1,3}, Jaegul Choo^{1,3†}, Youngjae Yu^{2‡}

¹ KAIST AI ² Yonsei University ³ Letsur Inc.

{kangyeolk, wcho, jchoo}@kaist.ac.kr

{justin_seo, daniel5253, qhdamm23,

pikachuisabird, yjy}@yonsei.ac.kr

Abstract

Personalized text-to-image (P-T2I) generation aims to create new, text-guided images featuring the personalized subject with a few reference images. However, balancing the trade-off relationship between prompt fidelity and identity preservation remains a critical challenge. To address the issue, we propose a novel P-T2I method called **Layout-and-Retouch**, consisting of two stages: 1) *layout generation* and 2) *retouch*. In the first stage, our step-blended inference utilizes the inherent sample diversity of vanilla T2I models to produce diversified layout images, while also enhancing prompt fidelity. In the second stage, multi-source attention swapping integrates the context image from the first stage with the reference image, leveraging the structure from the context image and extracting visual features from the reference image. This achieves high prompt fidelity while preserving identity characteristics. Through our extensive experiments, we demonstrate that our method generates a wide variety of images with diverse layouts while maintaining the unique identity features of the personalized objects, even with challenging text prompts. This versatility highlights the potential of our framework to handle complex conditions, significantly enhancing the diversity and applicability of personalized image synthesis.

1 Introduction

Following the notable success of text-to-image (T2I) generation models, *e.g.*, Stable Diffusion [40], which are trained on large-scale datasets of text-image pairs, there has been increasing interest in personalized text-to-image (P-T2I) generation problems [11]. Given a few reference images containing a specific subject, P-T2I models aim to create new, prompt-guided images that include the personalized subject. To effectively achieve this goal, previous studies [11, 42, 30] proposed to learn new personalized concepts by adjusting pre-trained T2I generation models [40, 36]. These methods have demonstrated promising and visually satisfactory results, leading to the development of versatile applications with practical potential in real-world situations.

When evaluating P-T2I models, there exist two primary criteria. 1) *Prompt fidelity* examine the extent to which the generated image aligns with the textual description. 2) On the other hand, *identity preservation* assesses whether the appearance of a subject within the image faithfully maintains the characteristics of the personalized subject. In essence, a trade-off relationship may exist between prompt fidelity and identity preservation [27], thereby P-T2I models often miss to illustrate characteristics of personalized concept when it comes to strictly following prompt guidance as well as retaining the details of visual attributes of the concept [34, 16].

* These authors contributed equally to this work.

† Co-corresponding authors

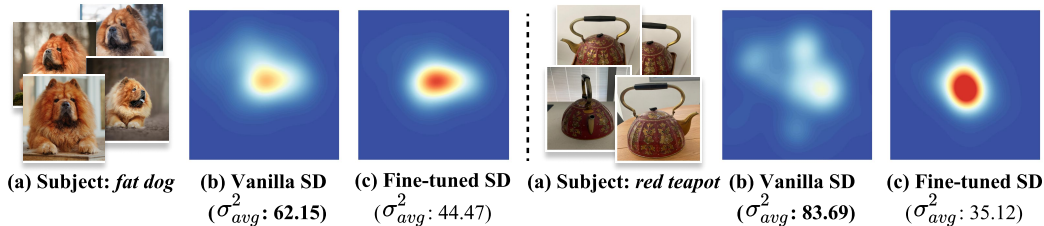


Figure 1: Visualizations of center-point distributions of subjects. Using the ViCo [16] evaluation prompt, we generate 10 images per prompt with both Stable Diffusion (SD) [40] and Dreambooth [42] trained with (a) the subject of reference images. For each subject, we locate the bounding box of an object. We then compute the 2D center-point distribution by fitting Gaussian distributions to each center point, with the mean being the center point itself and the variance fixed, and then normalize all distributions. (b) Vanilla SD places objects across a wider range compared to (c) fine-tuned SD, indicating that fine-tuned SD has a weaker ability to generate a diverse range of image layouts. σ_{avg}^2 denotes the averaged *variances* of 2D center points, meaning that the center point set is more widely dispersed with vanilla SD.

Since preserving the identity of each subject is crucial in P-T2I problems, a line of research [22, 45, 47, 5, 34, 53] has focused on maintaining visual appearance during the inference phase by explicitly using reference images as an additional condition. Although these approaches enhance the identity preservation capabilities of P-T2I models, they do not improve prompt fidelity. This is because the ability to generate contextually appropriate images is inherently limited by the intrinsic capacities of the pre-trained P-T2I model. To investigate the inherent limitations of pre-trained P-T2I generation models in comparison with vanilla T2I models such as Stable Diffusion [40], we conduct exploratory experiments, the results of which are shown in Fig. 1. In fact, requiring the P-T2I model to depict the appearance of personalized concepts and synthesize non-personalized contexts is highly demanding.

To overcome the limitations of the previous works and generate personalized images from diverse and challenging prompts while retaining identity characteristics, we propose a novel off-the-shelf P-T2I generation strategy called **Layout-and-Retouch**. Our core idea involves separating the generation of non-personalized parts (e.g., background and wearables) from the identity of target subjects, thus structuring our generation process into two stages: 1) *layout image generation* and 2) *retouch*.

In the layout image generation stage, we primarily focus on improving prompt fidelity, irrespective of identity preservation. Specifically, our first aim is to create a layout image that provides structural guidance for the next step. For this purpose, we carefully design a **step-blended denoising** approach to improve the prompt fidelity of pre-trained P-T2I models by leveraging the diverse expressive capabilities of vanilla T2I generation models. As a result, we obtain layout image features that depict an object visually resembling the target subject, occupying a specific position within the image. The remaining areas are arranged to align with the provided textual prompt.

In the retouch stage, the remaining goal is to precisely calibrate the target subject while preserving the background context of the layout image obtained in the previous stage. To achieve this, we propose **multi-source attention swap**, a straightforward yet effective method that integrates context from the layout image and captures detailed visual appearance from a reference image simultaneously. The principle of the attention swap technique is to transmit information, such as object appearance and style, from reference visual characteristics by replacing the queries, keys, and values in the target denoising steps with those derived from a reference image [5, 12, 13, 9].

Our two-stage method enables the creation of personalized images with diversified layouts, surpassing existing methods in variety. Extensive experiments demonstrate its capability to produce diverse images and effectively manage challenging prompts.

2 Related Work

2.1 Text-Guided Image Generation and Editing

T2I generation models. T2I generation models [51, 35, 38, 40, 43, 36] have been extensively studied for their ability to create realistic images from textual descriptions. Recently, diffusion-based

models [38, 40, 43] have demonstrated significant success in producing photo-realistic images from user-provided text, offering exceptional controllability. However, models such as Imagen [43], Stable Diffusion [40], and DALL-E series [39, 38, 3], still face challenges in generating personalized images. Specifically, these models struggle when it comes to creating images based on specific or user-defined concepts, where the identities are difficult to accurately convey through text descriptions.

Text-guided image editing. Building on the advancements in T2I generation models, there have been active studies in editing specific images based on text inputs [28, 32, 18, 2, 4, 24, 23, 1]. However, editing images while retaining most of the original content is challenging, as even minor modifications to the text guidance can lead to significant changes. Therefore, early works such as SDEdit [32] and Blended-Diffusion [1] have been developed with limited image editing capabilities, *e.g.*, requiring users to provide a spatial mask to specify the area for editing. To address these limitations, Imagic [23] and InstructPix2Pix [4] have been designed using multi-stage training processes and multiple distinct models, respectively. Despite their effectiveness, these editing models may not guarantee identity preservation when performing complex text-driven image transformations.

2.2 Text-to-Image Personalization

Addressing the limitations of T2I generation and editing models, personalization models aim to create new images using a few images of an object, while preserving the object’s identity consistently.

Optimization-based methods. Previous studies [11, 42, 26, 15, 49, 16, 8, 48, 14] have explored generating consistent image variations of a specified concept by embedding the concept within the textual domain of diffusion-based models, often represented by a particular token. This approach allows for the controlled generation of images that align closely with a target prompt. Textual Inversion [11] and DreamBooth [42] are advanced methods for creating personalized images through diffusion-based models. Textual Inversion optimizes a textual embedding to integrate a specialized token with the target prompt, while DreamBooth extends this by adjusting all parameters of the denoising U-Net, targeting a specific token and the subject’s class category. These methods enhance the precision and contextual relevance of image generation. Research efforts have continually advanced by focusing on tuning key components, such as the cross-attention layer [26, 15, 48], or by incorporating additional adapters [16] to enhance training efficiency and conditioning performance. While these studies have shown promising results, they have faced limitations in preserving the appearance of subjects.

Off-the-shelf methods. To eliminate the necessity of additional fine-tuning steps, researchers have explored plug-in T2I personalization techniques [5, 33, 10, 29, 53, 46, 19]. These approaches not only enhance computational efficiency but also improve outcomes by explicitly utilizing reference images as an additional condition to capture visual appearance during the inference phase. Technically, these methods manipulate the keys and values of the self-attention module during the denoising process of the U-Net, effectively altering structures and textures [5, 34]. MasaCtrl [5], for instance, employs a dual-path pipeline that synthesizes both a reference and a target image concurrently, replacing the target’s keys and values in the self-attention module with those from the reference. More recently, DreamMatcher [34] introduced a technique that adjusts these replaced target values using flowmap-based semantic matching to ensure structural correspondences between the target and reference latent features. However, the P-T2I model alone may present significant limitations in generating diverse layout images, often making it difficult to handle complex prompt conditions. To overcome this issue, we propose a two-stage framework, Layout-and-Retouch, where the vanilla T2I model is responsible for constructing an initial layout, leading to improvements in both prompt fidelity and layout diversity.

3 Proposed Methods

3.1 Preliminaries

Latent diffusion model. Recent advancements in text-to-image diffusion models, such as Stable Diffusion [40], have achieved robust and efficient image generation by performing the denoising process within the latent space using a pre-trained autoencoder. Specifically, a pre-trained encoder compresses an image into a latent representation \mathbf{z} , followed by diffusion and iterative denoising steps using a conditional diffusion model ϵ_θ . During denoising, a text condition \mathbf{y} is incorporated through a cross-attention module, guiding the latent representations to align with the text condition. The training objective is formulated as

$$\mathcal{L} = \mathbb{E}_{\mathbf{y}, \mathbf{z}, \epsilon, i} [\|\epsilon - \epsilon_\theta(\mathbf{z}^i, i, \text{CLIP}(\mathbf{y}))\|], \tag{1}$$

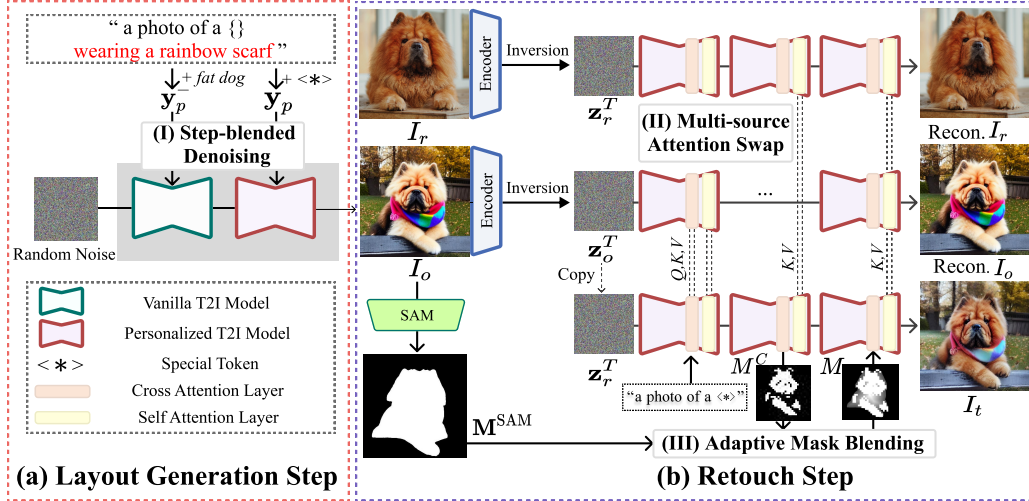


Figure 2: Overall pipeline of Layout-and-Retouch: (a) In the layout generation step, we perform (I) step-blended denoising using vanilla and personalized T2I models. Different subject-related words (e.g., red vase and $\langle * \rangle$) are fed to each model. (b) The retouch step focuses on calibrating the target subject while maintaining the layout image structure. This is achieved using (II) multi-source attention swap, where intermediate variables from the attention layers of other denoising paths are used to create the target image, and (III) adaptive mask blending, which combines M^{SAM} and a cross-attention map to generate an accurate mask for blending feature maps in the self-attention layer.

where $\epsilon \sim \mathcal{N}(0, 1)$, CLIP denotes the text encoder of CLIP [37], and \mathbf{z}^i denotes a noisy version of the latent representations \mathbf{z} . Also, discrete time steps i are sampled from the set $\{1, \dots, T\}$ uniformly at random. For effective and robust image generation, we base our method on Stable Diffusion [40].

The latent diffusion model employs a time-conditional U-net backbone, which features multiple self-attention and cross-attention layers. Formally, the attention mechanism can be written as

$$\text{Attention}(Q, K, V) = \text{Softmax} \left(\frac{QK^T}{\sqrt{d}} V \right),$$

where Q represents the query encoded using latent feature maps, while K and V denote the key and value, respectively. These are encoded using either the latent feature maps for self-attention layers or textual embeddings for cross-attention layers.

Pre-training personalized model. In general, training a personalized model requires a set of m reference images $\{I_r^m\}_{m=1}^M$ that describe a target concept [11, 42, 8]. Previous approaches fine-tune either a partial [11] or the entire network [42] to encapsulate the target concept into the network. After training, special text tokens such as " $\langle * \rangle$ " are used to represent the personalized information, which can be flexibly combined with additional text conditions. Although pre-trained networks with the special text tokens have shown a remarkable capacity to convey the target object, the use of only a few training images makes them highly susceptible to overfitting [52, 54, 7]. One of our observations is that a pre-trained personalized model has weak capacities for generating images with diverse configurations as shown in Fig. 1. Throughout this paper, we denote the text condition incorporating the special text token as \mathbf{y}_p , while the text condition with only the special text token removed is denoted as \mathbf{y}_p^- . Additionally, we define a neutral text condition, which includes only the concept without any specific text guidance, as \mathbf{y}_r (e.g., a photo of $\langle * \rangle$).

3.2 Layout-and-Retouch Framework

Given a reference image I_r and the corresponding text condition \mathbf{y}_p , our goal is to generate a target image I_t that adheres to the text condition while retaining the appearance of I_r . One solution might be to leverage a pre-trained P-T2I model with \mathbf{y}_p ; however, we find that the pre-trained P-T2I model tends to synthesize images within a restricted layout space (See Fig. 1 and Fig 4). We hypothesize that

the model pre-trained on repetitive layouts limits its capabilities to generate diverse configurations. To address this issue, we propose the Layout-and-Retouch framework, as depicted in Fig. 2.

3.2.1 Stage 1 - Layout Generation

Step-blended denoising. Our core idea is to utilize the expressiveness of vanilla Stable Diffusion (SD) [40] by having it create the layout in the initial steps. Delegating the task of generating the initial layout to vanilla SD broadens the range and expressiveness of the layouts. We use the text condition y_p^- since vanilla SD lacks prior knowledge of the concept. As shown in Fig. 1, layouts generated by vanilla SD are more diverse than those from pre-trained P-T2I models. By leveraging vanilla SD’s ability to generate diverse initial layouts, we facilitate the creation of a broader spectrum of layout images. The initial layout generation is achieved within λ_1 steps, determined based on empirical studies. Detailed results and analysis of these λ_1 iterations are in the Appendix.

Generating the initial layouts within λ_1 steps, the subsequent steps adjust the initial object appearance to visually align with the target subject while preserving the initial structure. We use y_p and the personalized model for the remaining steps. Let ϵ_θ and ϵ_θ^* represent the vanilla and personalized denoising networks, respectively, and let z^i denote the latent representations at each denoising step i . Formally, computing the latent representations in step-blended denoising can be written as:

$$z_{i-1} = \begin{cases} \text{Sample}(z^i, \epsilon_\theta(z^i, y_p^-, i)) & \text{if } i < \lambda_1, \\ \text{Sample}(z^i, \epsilon_\theta^*(z^i, y_p, i)) & \text{otherwise,} \end{cases} \quad \text{for } i = T, T-1, \dots, 1,$$

where `Sample` operation determines the next latent representations using a predicted noise. Following the denoising steps, a decoding process is performed to generate a layout image I_o .

3.2.2 Stage 2 - Retouch

Multi-source attention swap. Although a layout image I_o captures some visual characteristics of the target subject, it loses finer details. To enhance the details, we use attention swapping techniques [5, 12] with multiple source images: I_o and I_r . Specifically, intermediate variables from cross and self-attention modules derived from I_o and I_r are passed to the denoising steps of I_t . We denote the queries, keys, and values of the cross-attention module as Q_t^c, K_t^c, V_t^c and those of the self-attention module as Q_t^s, K_t^s, V_t^s in the target denoising process. Additionally, we use y_r as a text condition to focus on modifying the visual features of the target object throughout the denoising process.

Algorithm 1 describes an overall process of the Retouch stage. During the target path denoising, attention swapping replaces Q_t^c, K_t^c, V_t^c or Q_t^s, K_t^s, V_t^s with variables from the layout and context path. In the early steps, we use Q_o^c, K_o^c, V_o^c and Q_o^s, K_o^s, V_o^s from the layout path, integrating them into the target path to construct the overall structure of the noisy image. This sharing helps I_t loosely adhere to I_o ’s structure, making replication easier. In later denoising steps, K_r^s and V_r^s from the reference path replace those in the target path to infuse detailed features from the reference object. Additionally, a composite foreground mask \mathbf{M} combines latent representations of the target and layout path within a self-attention layer, where the details on \mathbf{M} are provided below.

Adaptive mask blending. To enhance the visual details of the target subject, we explicitly create a foreground mask to directly blend latent representations of the layout image. One can make foreground masks using cross-attention maps that correlate to the object prompt tokens extracted from the decoder as in [5], where the maps are averaged and then thresholded to produce a binary mask $\mathbf{M}^c \in \mathbb{R}^{h \times w}$, where h and w represent the spatial dimensions of the latent representations. However, we observe that \mathbf{M}^c often fail to cover the entire foreground and includes noisy regions. To mitigate this issue, we additionally harness a binary foreground mask $\mathbf{M}^{\text{SAM}} \in \mathbb{R}^{H \times W}$ where H, W denote height and width respectively computed by Segment-Anything [25] given a layout image. We also notice that only using \mathbf{M}^{SAM} results in layout-target misalignment, since detailed appearance or locations may shift during the target generation process (details are explained in the Appendix C.2). Therefore, we propose an adaptive mask blending technique to mitigate these issues.

Let $\mathbf{M}[x, y]$ be the value at position (x, y) and $\text{Resize}(\mathbf{M}^c) \in \mathbb{R}^{H \times W}$ be the resized mask from the averaged cross-attention map. We first discard noisy regions of \mathbf{M}^c based on \mathbf{M}^{SAM} , i.e.,

$$\mathbf{M}^k[x, y] = \text{OR}(\text{Resize}(\mathbf{M}^c)[x, y], \mathbf{M}^{\text{SAM}}[x, y]),$$

Algorithm 1 Retouch stage with multi-source attention swapping algorithm

```
1: Inputs: layout image  $I_o$ , reference image  $I_r$ , neutral text condition  $\mathbf{y}_r$ , target text condition  $\mathbf{y}_p$  SAM mask  $\mathbf{M}^{\text{SAM}}$ , pre-trained personalized diffusion model  $\epsilon_\theta^*$ 
2:  $\mathbf{z}_r^T \leftarrow \text{DDIMInversion}(\text{Encoder}(I_r), \text{""})$  ▷ DDIM inversion for reference image
3:  $\mathbf{z}_o^T \leftarrow \text{DDIMInversion}(\text{Encoder}(I_o), \text{""})$  ▷ DDIM inversion for layout image
4:  $\mathbf{z}_t^T \leftarrow \mathbf{z}_o^T$  ▷ Initialize target latent with layout latent
5: for  $i = T, T - 1, \dots, 1$  do
6:    $\{Q_r^s, K_r^s, V_r^s\}, \epsilon_r \leftarrow \epsilon_\theta^*(\mathbf{z}_r^i, \mathbf{y}_r, i)$  ▷ Reference path
7:    $\{Q_o^c, K_o^c, V_o^c\}, \{Q_o^s, K_o^s, V_o^s\}, \phi_o \leftarrow \epsilon_\theta^*(\mathbf{z}_o^i, \mathbf{y}_p, i)$  ▷ Layout path
8:    $\{Q_t^c, K_t^c, V_t^c\}, \{Q_t^s, K_t^s, V_t^s\} \leftarrow \epsilon_\theta^*(\mathbf{z}_t^i, \mathbf{y}_r, i)$  ▷ Target path
9:   if  $i > \lambda_2$  then
10:      $\epsilon^* \leftarrow \epsilon_\theta^*(\mathbf{z}_t^i, \mathbf{y}_r, i, \{Q_o^c, K_o^c, V_o^c\}, \{Q_o^s, K_o^s, V_o^s\})$  ▷ Denoise w/ variables
11:   else
12:      $\epsilon^* \leftarrow \epsilon_\theta^*(\mathbf{z}_t^i, \mathbf{y}_r, i, \{Q_t^c, K_t^c, V_t^c\}, \{Q_t^s, K_t^s, V_t^s\}, \phi_o, \mathbf{M}^{\text{OURS}})$  ▷ Denoise w/ variables and mask
13:   end if
14:    $\mathbf{z}_r^{i-1} \leftarrow \text{Sample}(\mathbf{z}_r^i, \epsilon_r)$  ▷ Sample next latent for reference image
15:    $\mathbf{z}_o^{i-1} \leftarrow \text{Sample}(\mathbf{z}_o^i, \epsilon_o)$  ▷ Sample next latent for layout image
16:    $\mathbf{z}_t^{i-1} \leftarrow \text{Sample}(\mathbf{z}_t^i, \epsilon^*)$  ▷ Sample next latent for target image
17: end for
18:  $I_t = \text{Decoder}(\mathbf{z}_t^0)$ 
19: return  $I_t$ 
```

where OR represents pixel-wise operations between two binary values. Then, we apply a distance transformation [41] to smooth the abrupt transitions between regions with values of 1 and regions with values of 0. Lastly, we add the area with 1s of \mathbf{M}^c to explicitly insert confident regions based on the activated values of \mathbf{M}^c . Formally, this can be formulated as follows:

$$\mathbf{M}[x, y] = \text{Normalize}(\mathcal{D}_{l_2}(\mathbf{M}^k[x, y])) + \mathcal{C}(\mathbf{M}^c[x, y]),$$

where \mathcal{D}_{l_2} denotes the distance transformation using l_2 -distance and Normalize is a scaling operation to map the values to the range [0.5, 1.0]. Also a small connected set removal operation \mathcal{C} performs to discard noisy pixel mask areas by removing connected sets below a specified volume threshold. This allows us to reduce the potential negative effects caused by noisy masks.

During denoising steps, $\mathbf{M} \in \mathbb{R}^{H \times W}$ is resized to match the spatial dimension of the latent representations. To blend the latent representations between the target and layout path, weighted summation is performed in the self-attention layer:

$$\phi^* = \mathbf{M} \odot \phi_t + (1 - \mathbf{M}) \odot \phi_o,$$

where \odot represents an element-wise multiplication, and ϕ_t, ϕ_o are the output latent representations of the self-attention layer, for the target and layout path, respectively. The combined latent representation ϕ^* is passed to the next layer after the self-attention layer.

4 Experiments

In this section, we describe the experimental setup (Section 4.1), including benchmark datasets, baselines, and evaluation metrics to evaluate Layout-and-Retouch and baselines in three aspects:

1. **Layout Diversity:** To assess the model’s ability to generate diverse layouts.
2. **Identity Preservation:** To ensure that objects consistently maintain their detailed characteristics across images.
3. **Prompt Fidelity:** To verify that the outputs faithfully adhere to the text guidance.

Comparisons with baselines include both quantitative and qualitative analyses to investigate the add-on effects of Layout-and-Retouch and to compare it with various baselines according to the criteria mentioned above (Section 4.2). The qualitative analysis includes experimental results validating the superiority of Layout-and-Retouch in generating diverse images, along with an ablation study demonstrating the contribution of each component of the proposed method. (Section 4.3)



Figure 3: Qualitative comparisons with *challenging* prompts. Our method produces images with poses and scales significantly different from the reference images compared to other methods. Additionally, it excels at generating images that accurately follow challenging prompts. It is noteworthy that our method does not produce images with identical structures, benefiting from step-blended denoising.

4.1 Experimental Setup

Datasets. We adopt the image-prompt dataset proposed in ViCo [16] for evaluation as a *normal* dataset. This dataset includes 16 unique concepts from previous methods [11, 42, 26] and contains 31 distinct prompts. The categories include 5 live animals, 6 toys, 3 household goods, 1 accessory, and 1 building, with 4-7 images per object. The evaluation prompt set, with 31 prompts, is referenced from Dreambooth [42] and covers both living and non-living entities, including a few type-specific prompts. Additionally, we use the *challenging* prompt dataset proposed in DreamMatcher [34], which includes 24 prompts requiring large displacement or complex scene synthesis. For evaluation, we generate 8 images per object and prompt, following the evaluation protocols of previous studies [16, 34].

Baselines. Our proposed approach is compatible with *any* P-T2I model without requiring additional training process. The primary baselines are the original P-T2I models such as Textual inversion [11], Dreambooth [42], Custom diffusion [26] to evaluate potential performance improvements. Furthermore, we compare our method with other tuning-free plug-in baselines such as FreeU [46], MagicFusion [53] and DreamMatcher [34]. As a backbone algorithm for evaluating plug-in baselines, we use Textual Inversion [11] and DreamBooth [42] as a personalized model for all baselines, including our method.

Evaluation metrics. Following conventional work [11, 42, 26, 16], we focus on measuring two primary aspects: (1) identity preservation and (2) prompt fidelity. To evaluate identity preservation, we adopt I_{CLIP} and I_{DINO} , which respectively employ CLIP [37] and DINO [6] as backbone networks to measure subject similarity between $\{I_r^m\}_{m=1}^M$ and the generated images. For evaluating prompt fidelity, we utilize the CLIP [37] image and text encoder to compute text-image similarity score, denoted as T_{CLIP} . Lastly, we utilize Inception Score (IS) [44] to measure the diversity of the generated image set.

Methods	Normal Prompts			Challenging Prompts		
	I _{DINO} ↑	I _{CLIP} ↑	T _{CLIP} ↑	I _{DINO} ↑	I _{CLIP} ↑	T _{CLIP} ↑
DreamMatcher [34]	0.576	0.781	0.278	0.650	0.824	0.310
MagicFusion [53]	0.521	0.759	0.278	0.599	0.801	0.315
FreeU [46]	0.526	0.770	0.281	0.587	0.795	0.312
Ours	0.600	0.789	0.297	0.665	0.824	0.315

Table 1: Quantitative comparison against various plug-in based models [46, 53, 34] on base prompts curated by ViCo [16]. We used Textual Inversion [11] for normal prompts baseline, and we used Dreambooth [42] for challenging prompts baseline.

4.2 Comparisons with Baselines

Comparisons with plug-in baselines We compare our approach with tuning-free plug-in baselines: FreeU [46], MagicFusion [53] and DreamMatcher [34] on both normal and challenging prompts. Fig. 3 shows visual comparisons of Layout-and-Retouch and baseline outputs. As seen, the proposed method successfully follows challenging prompt guidance while dynamically adapting the personalized object.

As shown in Table 1 (Left), the proposed method shows superior and comparable performances on both normal prompts and challenging prompts. For *normal* prompts, our method presents consistent performance increases in I_{DINO}, I_{CLIP} and T_{CLIP}. These improvements emphasize the effectiveness of our method in achieving both goals of personalized image generation: identity preservation and prompt fidelity. Evaluation on *challenging* prompts is shown in Table 1 (Right). Although, baseline models show comparable results on T_{CLIP}, the I_{DINO} and I_{CLIP} scores indicate that the prompt condition for generating personalized objects is not being successfully fulfilled. Meanwhile, our approach effectively balances the dual objectives of identity preservation and prompt fidelity in the generated images.

We conduct a user study to evaluate three aspects: (1) Identity preservation, (2) Prompt fidelity, and (3) Diversity. As can be seen in the ranking score of Table 3, our approach is largely preferred against the other plug-in baselines. In the diversity aspect, we outperform DreamMatcher [34] by a large margin, demonstrating strength in generating diverse images. The user study setup is written in Appendix B.4.

Methods	I _{DINO} ↑	I _{CLIP} ↑	T _{CLIP} ↑	Ranking Score	Identity Preservation	Prompt Fidelity
Textual Inversion	0.527	0.769	0.277		0.194	0.175
+ Ours	0.600 (+13.9%)	0.789 (+2.6%)	0.297 (+7.2%)			
Dreambooth	0.637	0.814	0.313		0.203	0.183
+ Ours	0.655 (+2.8%)	0.815 (+0.1%)	0.317 (+1.3%)		0.225	0.252
Custom Diffusion	0.658	0.814	0.315		0.377	0.389
+ Ours	0.659 (+0.2%)	0.814 (+0.0%)	0.317 (+0.6%)	WinRate (Diversity)	Ours 77.9%	DreamMatcher 22.1%

Table 2: Add-on effects of our method. Our method consistently improve baselines, validating the effectiveness of the proposed approach. Performance gains are marked in blue. Table 3: User study results against plug-in baselines. Performance gains are marked in blue.

Improving P-T2I baselines. We validate the effectiveness of our proposed framework by integrating it with Textual inversion [11], Dreambooth [42], Custom diffusion [26]. Table 2 presents the performance evaluations for identity preservation and prompt fidelity. As shown, our approach enhances prompt fidelity across all baselines while maintaining comparable results in identity preservation. Notably, the significant and consistent improvements in prompt fidelity demonstrate the effectiveness of our method, highlighting the importance of initial layouts in generating prompt-aligned images. We present more qualitative comparisons with P-T2I baselines in the Appendix C.3.

4.3 Qualitative Analysis

Analysis on image diversity. One of the strengths of the proposed method lies in synthesizing images with diverse layouts. To demonstrate this, we measure the diversity of the generated images with DreamMatcher [34] and our approach, employing the diversity metric IS score [44]. Instead of generating a small set across all prompts, we generate 400 images for 10 randomly sampled

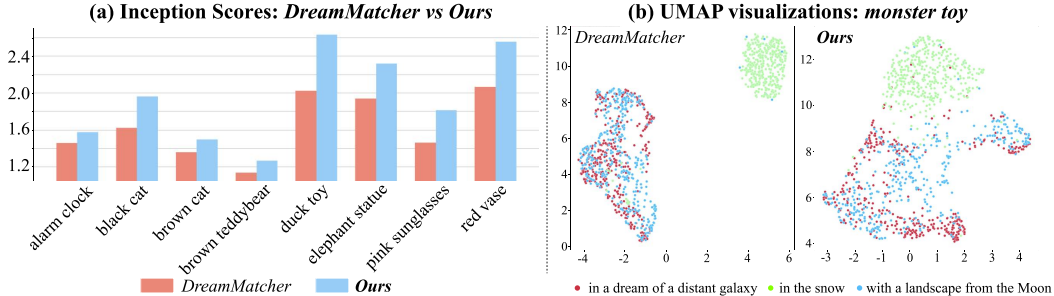


Figure 4: Illustrations of diversity analysis. (a) We measure the IS score across individual objects, and verifying our method has a strong tendency to generate more diverse images. (b) Our methodology is distributed more broadly within the same prompt. This means that our approach is capable of generating images with diverse configurations.

prompts out of the 31 available for each of the 8 objects with the aim of faithfully measuring the score. As seen in Fig. 4 (a), our method surpasses DreamMatcher [34] in terms of IS score across all objects, indicating the superiority of ours to create images with diverse configurations. In addition, we evaluate the diversity of the generated images by projecting three image groups of prompt using pre-trained ResNet [17], then apply UMAP [31] to visualize the embedding space. As shown in Fig. 4 (b) visualizes of clusters, our method obviously produces the images in broader coverage compared to DreamMatcher [34]. This proves the strength of Layout-and-Retouch in generating diverse and prompt-aligned images. The sampled prompts list is available in the Appendix 6.

	Configurations	$I_{DINO} \uparrow$	$I_{CLIP} \uparrow$	$T_{CLIP} \uparrow$
(I)	Dreambooth [42]	0.637	0.814	0.313
(II)	(I) + Step-blended denoising	0.620	0.802	0.319
(III)	(II) + Reference attention swap	0.707	0.812	0.280
(IV)	(II) + Multi-source attention swap	0.615	0.798	0.320
(V)	(IV) + Adaptive mask blending (<i>Ours</i>)	0.655	0.815	0.317

Table 4: Performances of various configurations on ViCo [16] dataset.

Ablation study. We study the contribution of each component by sequentially adding step-blended denoising, multi-source attention swap, and adaptive mask blending. An ablation study is conducted based on Dreambooth baseline [42]. Table 4 shows the performances of different configurations in aspects of identity preservation (I_{DINO} , I_{CLIP}) and prompt fidelity (T_{CLIP}). (II) Building upon Dreambooth [42], we introduce step-blended denoising, and demonstrate a significant enhancement in prompt fidelity. (III) A natural extension is to incorporate a reference image into the denoising path by utilizing the corresponding K and V from the self-attention layer derived from the reference image denoising process. However, we observe a significant degradation in prompt fidelity, primarily due to the increased complexity of generating a background while accurately reflecting the visual characteristics of the reference image. (IV) To address this, we adopt a two-stage framework with multi-source attention swapping. This method achieves a significant performance boost in prompt fidelity compared to (III), but it leads to a reduction in identity preservation. (V) In response, we employ adaptive mask blending, which enhances identity preservation and produces superior results in both identity preservation and prompt fidelity.

5 Conclusion

In this paper, we present Layout-and-Retouch, a two-stage framework for creating personalized images with prompt-aligned, diverse configurations. Our motivation stems from preliminary observations on the limited layout generation capacity, which results in a weak ability to handle *challenging* prompts. To address this issue, we introduce the *step-blended denoising* to diversify image layouts by leveraging the expressive power of the vanilla T2I model. Furthermore, we propose the *multi-source attention swap* and *adaptive mask blending* to faithfully transfer the visual features of the reference image while preserving the layout image structure. The combination of these modules enables our

framework to effectively enrich image layouts, thereby improving its ability to handle challenging prompts. Extensive experiments demonstrate the superiority of Layout-and-Retouch in generating diverse prompt-aligned images, particularly in handling challenging prompts compared to baselines.

References

- [1] Omri Avrahami, Dani Lischinski, and Ohad Fried. Blended diffusion for text-driven editing of natural images. In *Proceedings of the IEEE/CVF Conference on Computer Vision and Pattern Recognition*, pages 18208–18218, 2022.
- [2] Omer Bar-Tal, Dolev Ofri-Amar, Rafail Fridman, Yoni Kasten, and Tali Dekel. Text2live: Text-driven layered image and video editing. In *European conference on computer vision*, pages 707–723. Springer, 2022.
- [3] James Betker, Gabriel Goh, Li Jing, Tim Brooks, Jianfeng Wang, Linjie Li, Long Ouyang, Juntang Zhuang, Joyce Lee, Yufei Guo, et al. Improving image generation with better captions. *Computer Science*. <https://cdn.openai.com/papers/dall-e-3.pdf>, 2(3):8, 2023.
- [4] Tim Brooks, Aleksander Holynski, and Alexei A Efros. Instructpix2pix: Learning to follow image editing instructions. In *Proceedings of the IEEE/CVF Conference on Computer Vision and Pattern Recognition*, pages 18392–18402, 2023.
- [5] Ming Cao, Xintao Wang, Zhongang Qi, Ying Shan, Xiaohu Qie, and Yinqiang Zheng. Masactrl: Tuning-free mutual self-attention control for consistent image synthesis and editing. *2023 IEEE/CVF International Conference on Computer Vision (ICCV)*, pages 22503–22513, 2023.
- [6] Mathilde Caron, Hugo Touvron, Ishan Misra, Hervé Jégou, Julien Mairal, Piotr Bojanowski, and Armand Joulin. Emerging properties in self-supervised vision transformers. In *Proceedings of the IEEE/CVF international conference on computer vision*, pages 9650–9660, 2021.
- [7] Daewon Chae, Nokyung Park, Jinkyu Kim, and Kimin Lee. Instructbooth: Instruction-following personalized text-to-image generation. *arXiv preprint arXiv:2312.03011*, 2023.
- [8] Hong Chen, Yipeng Zhang, Xin Wang, Xuguang Duan, Yuwei Zhou, and Wenwu Zhu. Disenbooth: Disentangled parameter-efficient tuning for subject-driven text-to-image generation. *arXiv preprint arXiv:2305.03374*, 2023.
- [9] Jiwoo Chung, Sangeek Hyun, and Jae-Pil Heo. Style injection in diffusion: A training-free approach for adapting large-scale diffusion models for style transfer. *arXiv preprint arXiv:2312.09008*, 2023.
- [10] Xiaoyue Duan, Shuhao Cui, Guoliang Kang, Baochang Zhang, Zhengcong Fei, Mingyuan Fan, and Junshi Huang. Tuning-free inversion-enhanced control for consistent image editing. In *Proceedings of the AAAI Conference on Artificial Intelligence*, volume 38, pages 1644–1652, 2024.
- [11] Rinon Gal, Yuval Alaluf, Yuval Atzmon, Or Patashnik, Amit H Bermano, Gal Chechik, and Daniel Cohen-Or. An image is worth one word: Personalizing text-to-image generation using textual inversion. *arXiv preprint arXiv:2208.01618*, 2022.
- [12] Jing Gu, Yilin Wang, Nanxuan Zhao, Tsu-Jui Fu, Wei Xiong, Qing Liu, Zhifei Zhang, He Zhang, Jianming Zhang, HyunJoon Jung, et al. Photoswap: Personalized subject swapping in images. *Advances in Neural Information Processing Systems*, 36, 2024.
- [13] Jing Gu, Yilin Wang, Nanxuan Zhao, Wei Xiong, Qing Liu, Zhifei Zhang, He Zhang, Jianming Zhang, HyunJoon Jung, and Xin Eric Wang. Swapanything: Enabling arbitrary object swapping in personalized visual editing. *arXiv preprint arXiv:2404.05717*, 2024.
- [14] Inhwa Han, Serin Yang, Taesung Kwon, and Jong Chul Ye. Highly personalized text embedding for image manipulation by stable diffusion. *arXiv preprint arXiv:2303.08767*, 2023.
- [15] Ligong Han, Yinxiao Li, Han Zhang, Peyman Milanfar, Dimitris Metaxas, and Feng Yang. Svdiff: Compact parameter space for diffusion fine-tuning. In *Proceedings of the IEEE/CVF International Conference on Computer Vision*, pages 7323–7334, 2023.
- [16] Shaozhe Hao, Kai Han, Shihao Zhao, and Kwan-Yee K Wong. Vico: Detail-preserving visual condition for personalized text-to-image generation. *arXiv preprint arXiv:2306.00971*, 2023.

- [17] Kaiming He, Xiangyu Zhang, Shaoqing Ren, and Jian Sun. Deep residual learning for image recognition. In *Proceedings of the IEEE conference on computer vision and pattern recognition*, pages 770–778, 2016.
- [18] Amir Hertz, Ron Mokady, Jay Tenenbaum, Kfir Aberman, Yael Pritch, and Daniel Cohen-Or. Prompt-to-prompt image editing with cross attention control. *arXiv preprint arXiv:2208.01626*, 2022.
- [19] Amir Hertz, Andrey Voynov, Shlomi Fruchter, and Daniel Cohen-Or. Style aligned image generation via shared attention. *arXiv preprint arXiv:2312.02133*, 2023.
- [20] Mengqi Huang, Zhendong Mao, Mingcong Liu, Qian He, and Yongdong Zhang. Realcustom: Narrowing real text word for real-time open-domain text-to-image customization. *arXiv preprint arXiv:2403.00483*, 2024.
- [21] Sangwon Jang, Jaehyeong Jo, Kimin Lee, and Sung Ju Hwang. Identity decoupling for multi-subject personalization of text-to-image models. *arXiv preprint arXiv:2404.04243*, 2024.
- [22] Xuhui Jia, Yang Zhao, Kelvin CK Chan, Yandong Li, Han Zhang, Boqing Gong, Tingbo Hou, Huisheng Wang, and Yu-Chuan Su. Taming encoder for zero fine-tuning image customization with text-to-image diffusion models. *arXiv preprint arXiv:2304.02642*, 2023.
- [23] Bahjat Kawar, Shiran Zada, Oran Lang, Omer Tov, Huiwen Chang, Tali Dekel, Inbar Mosseri, and Michal Irani. Imagic: Text-based real image editing with diffusion models. In *Proceedings of the IEEE/CVF Conference on Computer Vision and Pattern Recognition*, pages 6007–6017, 2023.
- [24] Gwanghyun Kim, Taesung Kwon, and Jong Chul Ye. Diffusionclip: Text-guided diffusion models for robust image manipulation. In *Proceedings of the IEEE/CVF Conference on Computer Vision and Pattern Recognition*, pages 2426–2435, 2022.
- [25] Alexander Kirillov, Eric Mintun, Nikhila Ravi, Hanzi Mao, Chloe Rolland, Laura Gustafson, Tete Xiao, Spencer Whitehead, Alexander C. Berg, Wan-Yen Lo, Piotr Dollár, and Ross Girshick. Segment anything. *arXiv:2304.02643*, 2023.
- [26] Nupur Kumari, Bingliang Zhang, Richard Zhang, Eli Shechtman, and Jun-Yan Zhu. Multi-concept customization of text-to-image diffusion. In *Proceedings of the IEEE/CVF Conference on Computer Vision and Pattern Recognition*, pages 1931–1941, 2023.
- [27] Kyungmin Lee, Sangkyung Kwak, Kihyuk Sohn, and Jinwoo Shin. Direct consistency optimization for compositional text-to-image personalization, 2024.
- [28] Bowen Li, Xiaojuan Qi, Thomas Lukasiewicz, and Philip HS Torr. Manigan: Text-guided image manipulation. In *Proceedings of the IEEE/CVF conference on computer vision and pattern recognition*, pages 7880–7889, 2020.
- [29] Henglei Lv, Jiayu Xiao, Liang Li, and Qingming Huang. Pick-and-draw: Training-free semantic guidance for text-to-image personalization. *arXiv preprint arXiv:2401.16762*, 2024.
- [30] Jiancang Ma, Junhao Liang, Chen Chen, and H. Lu. Subject-diffusion: Open domain personalized text-to-image generation without test-time fine-tuning. *ArXiv*, abs/2307.11410, 2023.
- [31] Leland McInnes, John Healy, and James Melville. Umap: Uniform manifold approximation and projection for dimension reduction. *arXiv preprint arXiv:1802.03426*, 2018.
- [32] Chenlin Meng, Yutong He, Yang Song, Jiaming Song, Jiajun Wu, Jun-Yan Zhu, and Stefano Ermon. Sdedit: Guided image synthesis and editing with stochastic differential equations. *arXiv preprint arXiv:2108.01073*, 2021.
- [33] Chong Mou, Xintao Wang, Jiechong Song, Ying Shan, and Jian Zhang. Dragondiffusion: Enabling drag-style manipulation on diffusion models. *arXiv preprint arXiv:2307.02421*, 2023.
- [34] Jisu Nam, Heesu Kim, DongJae Lee, Siyoon Jin, Seungryong Kim, and Seunggyu Chang. Dreammatcher: Appearance matching self-attention for semantically-consistent text-to-image personalization. *arXiv preprint arXiv:2402.09812*, 2024.
- [35] Alex Nichol, Prafulla Dhariwal, Aditya Ramesh, Pranav Shyam, Pamela Mishkin, Bob McGrew, Ilya Sutskever, and Mark Chen. Glide: Towards photorealistic image generation and editing with text-guided diffusion models. *arXiv preprint arXiv:2112.10741*, 2021.

- [36] Dustin Podell, Zion English, Kyle Lacey, Andreas Blattmann, Tim Dockhorn, Jonas Müller, Joe Penna, and Robin Rombach. SDXL: Improving latent diffusion models for high-resolution image synthesis. In *The Twelfth International Conference on Learning Representations*, 2024.
- [37] Alec Radford, Jong Wook Kim, Chris Hallacy, Aditya Ramesh, Gabriel Goh, Sandhini Agarwal, Girish Sastry, Amanda Askell, Pamela Mishkin, Jack Clark, et al. Learning transferable visual models from natural language supervision. In *International conference on machine learning*, pages 8748–8763. PMLR, 2021.
- [38] Aditya Ramesh, Prafulla Dhariwal, Alex Nichol, Casey Chu, and Mark Chen. Hierarchical text-conditional image generation with clip latents. *arXiv preprint arXiv:2204.06125*, 1(2):3, 2022.
- [39] Aditya Ramesh, Mikhail Pavlov, Gabriel Goh, Scott Gray, Chelsea Voss, Alec Radford, Mark Chen, and Ilya Sutskever. Zero-shot text-to-image generation. In *International conference on machine learning*, pages 8821–8831. Pmlr, 2021.
- [40] Robin Rombach, Andreas Blattmann, Dominik Lorenz, Patrick Esser, and Björn Ommer. High-resolution image synthesis with latent diffusion models. In *Proceedings of the IEEE/CVF conference on computer vision and pattern recognition*, pages 10684–10695, 2022.
- [41] Azriel Rosenfeld and John L Pfaltz. Distance functions on digital pictures. *Pattern recognition*, 1(1):33–61, 1968.
- [42] Nataniel Ruiz, Yuanzhen Li, Varun Jampani, Yael Pritch, Michael Rubinstein, and Kfir Aberman. Dreambooth: Fine tuning text-to-image diffusion models for subject-driven generation. In *Proceedings of the IEEE/CVF Conference on Computer Vision and Pattern Recognition*, pages 22500–22510, 2023.
- [43] Chitwan Saharia, William Chan, Saurabh Saxena, Lala Li, Jay Whang, Emily L Denton, Kamyar Ghasemipour, Raphael Gontijo Lopes, Burcu Karagol Ayan, Tim Salimans, et al. Photorealistic text-to-image diffusion models with deep language understanding. *Advances in neural information processing systems*, 35:36479–36494, 2022.
- [44] Tim Salimans, Ian Goodfellow, Wojciech Zaremba, Vicki Cheung, Alec Radford, and Xi Chen. Improved techniques for training gans. *Advances in neural information processing systems*, 29, 2016.
- [45] Jing Shi, Wei Xiong, Zhe Lin, and Hyun Joon Jung. Instantbooth: Personalized text-to-image generation without test-time finetuning, 2023.
- [46] Chenyang Si, Ziqi Huang, Yuming Jiang, and Ziwei Liu. Freeu: Free lunch in diffusion u-net. *arXiv preprint arXiv:2309.11497*, 2023.
- [47] Yu-Chuan Su, Kelvin CK Chan, Yandong Li, Yang Zhao, Han Zhang, Boqing Gong, Huisheng Wang, and Xuhui Jia. Identity encoder for personalized diffusion. *arXiv preprint arXiv:2304.07429*, 2023.
- [48] Yoad Tewel, Rinon Gal, Gal Chechik, and Yuval Atzmon. Key-locked rank one editing for text-to-image personalization. In *ACM SIGGRAPH 2023 Conference Proceedings*, pages 1–11, 2023.
- [49] Andrey Voynov, Qinghao Chu, Daniel Cohen-Or, and Kfir Aberman. $p+$: Extended textual conditioning in text-to-image generation. *arXiv preprint arXiv:2303.09522*, 2023.
- [50] Jiazheng Xu, Xiao Liu, Yuchen Wu, Yuxuan Tong, Qinkai Li, Ming Ding, Jie Tang, and Yuxiao Dong. Imagereward: Learning and evaluating human preferences for text-to-image generation. *Advances in Neural Information Processing Systems*, 36, 2024.
- [51] Tao Xu, Pengchuan Zhang, Qiuyuan Huang, Han Zhang, Zhe Gan, Xiaolei Huang, and Xiaodong He. Attngan: Fine-grained text to image generation with attentional generative adversarial networks. In *Proceedings of the IEEE conference on computer vision and pattern recognition*, pages 1316–1324, 2018.
- [52] Weili Zeng, Yichao Yan, Qi Zhu, Zhuo Chen, Pengzhi Chu, Weiming Zhao, and Xiaokang Yang. Infusion: Preventing customized text-to-image diffusion from overfitting. *arXiv preprint arXiv:2404.14007*, 2024.
- [53] Jing Zhao, Heliang Zheng, Chaoyue Wang, Long Lan, and Wenjing Yang. Magicfusion: Boosting text-to-image generation performance by fusing diffusion models, 2023.

- [54] Yufan Zhou, Ruiyi Zhang, Tong Sun, and Jinhui Xu. Enhancing detail preservation for customized text-to-image generation: A regularization-free approach. *arXiv preprint arXiv:2305.13579*, 2023.

In Appendix, we first discuss on broader impacts and limitations of the proposed method (Section A). Next, experimental details including implementation details are provided (Section B). Lastly, we present additional qualitative and quantitative analysis of our method(Section C). This includes in-depth visualizations of each component as well as further explanation about component. Furthermore, we present a user study to compare the effectiveness and user preferences compared to baselines.

A Discussion

A.1 Broader Impacts.

The proposed method can significantly enhance personalized image generation models, which may have various social impacts. Positively, it can facilitate the creation of more tailored and relevant content for individuals, improving user experiences across applications like social media, advertising, and digital art. Additionally, It can also assist in personalized education and training, providing custom visual aids suited to individual learning styles. However, there are potential risks, including the misuse of the technology for improving the quality of deepfakes or unauthorized digital impersonations, leading to privacy violations and misinformation. Ethical concerns also arise regarding the data used for personalization, especially if it involves sensitive or personal information. Therefore, ensuring transparency, obtaining consent, and implementing robust security measures are crucial to mitigate these risks.

A.2 Limitations.

While the proposed method shows promising performances in personalized image generation, it often fails to generate an user-intended image due to the reliance on vanilla Stable Diffusion (SD) model [40]. Specifically, a highly complicated prompt condition that is beyond the capacity of vanilla SD can cause a failure in the layout image, subsequently leading to undesirable target image. As seen in Fig. 5 (a), if the layout image does not adhere to prompt condition, the final output exhibits similar issues. Furthermore, the shape similarity between objects in layout and reference image would affect the identity preservation, as large shape discrepancies are difficult to rectify during the retouching stage. Fig. 5 (b) illustrates an example of generating with different layout images. As can be seen, retaining similar shapes is beneficial for creating a personalized object characteristics in later stage. We believe that using a more robust foundation model such as SDXL [36], to enhance prompt understanding and adherence on prompt conditions, is an effective approach to mitigating this problem. Our future plan includes utilizing SDXL as vanilla model in step-blended denoising and developing a technique to minimize shape difference.

B Experimental Details

B.1 Implementation Details

We use SD 1.4 [40] as our baseline vanilla foundation text-to-image model, and pre-training personalized models also are conducted based on SD 1.4. Specifically, we utilize all weights of personalized baseline models: Textual inversion [11], Dreambooth [42], Custom Diffusion [26] released in previous method [34]. In experiment, we use a DDIM sampler with a total inference time step to $T = 50$. Empirically, we set $\lambda_1 = 5$, $\lambda_1 = 3$ for normal and challenging prompt respectively and $\lambda_2 = 10$ for all datasets. Additionally, the mask blend operation starts from 31th to the last step. For our GPU setup, we use a NVIDIA GeForce RTX 3090 GPU for all experiments, which consumes about 18GiB memory during inference. It takes about 30 seconds for generating a single image including pre-processing. As for other parameters such as specific layers used for reference, we follow the prior works [5, 34].

B.2 Prompts for Diversity Experiment

Since one of our core claims is the diversity of synthesized images, we demonstrate our capabilities using a few different ways. First, we visualize the center point distributions of the target subjects (see Fig. 1), using all 31 prompts curated by ViCo [16] and generating 10 images per prompt. However, when measuring diversity using classic metrics such as Inception Score [44] or visualizing embedding

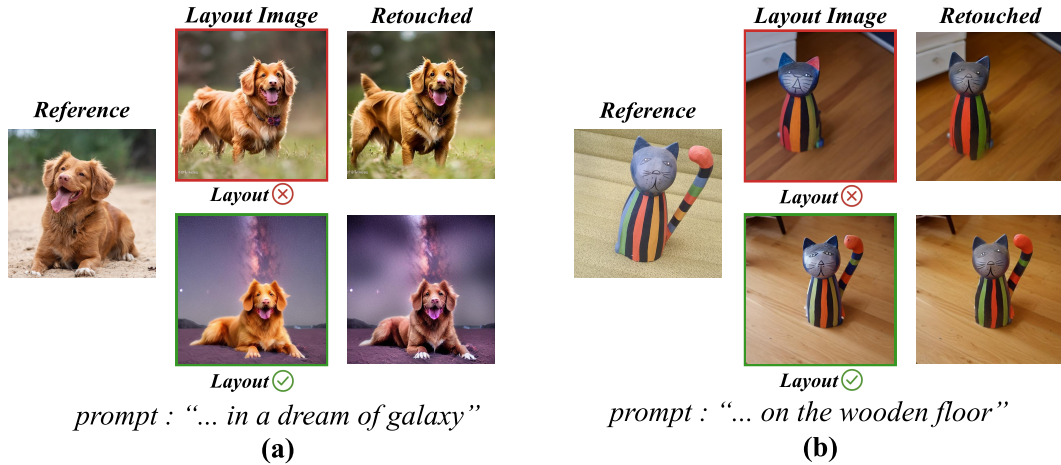


Figure 5: Layout Failure cases. (a) shows our generation results when layout fails to generate appropriate context, (b) shows when layout fails to faithfully generate shape of personalized concept. Since second stage of our pipeline lies on layout image, our pipeline can fail in prompts beyond the capacity of pre-trained SD backbone.

	Text prompts for non-live objects	Text prompts for live objects
Large displacement	a {} with the Eiffel Tower in the background	a {} with Japanese modern city street in the background
	a {} in a dream of a distant galaxy	a {} in a dream of a distant galaxy
	a {} with a beautiful sunset	a {} with a beautiful sunset
	a {} with a landscape from the Moon	a {} with a landscape from the Moon
Occlusion	a {} floating on top of water	a {} diving into a pool
	a {} nestled among rocks	a {} jumping over a fence
	a {} floating in a pond	a {} wearing a rainbow scarf
Novel-view synthesis	a {} on top of green grass with sunflowers around it	a {} in a police outfit
	a {} seen from the top	a {} seen from the top
	a {} seen from the side	a {} seen from the side

Figure 6: The list of 10 randomly sampled prompts that were used to generate images to compare the diversity of the output. We sampled the prompts according to the three different categories.

spaces [31], it is insufficient to generate only 10 samples with each prompt. Therefore, we randomly sample 10 prompts from three categories in total, from normal prompts and challenging prompts used in DreamMatcher [34]. These categories include large displacement, occlusion, and novel-view synthesis. We then generate 400 samples per prompt, resulting in a total of 4,000 images to evaluate Inception Scores for the objects depicted in Fig. 4. The list of prompts is provided in Fig. 6 below.

B.3 Analysis on evaluation metrics

Methods	T _{CLIP}	ImageReward
Textual Inversion	0.277	-0.975
+ Ours	0.297 (+7.2%)	-0.437 (+55.2%)
Dreambooth	0.313	0.255
+ Ours	0.317 (+1.3%)	0.420 (+64.7%)
Custom Diffusion	0.315	0.257
+ Ours	0.317 (+0.6%)	0.288 (+12.1%)

Table 5: The quantitative experimental results of evaluating the effect of our methodology in prompt fidelity, compared to the baseline optimization-based methods. We follow the dataset gathered by ViCo [16]. Performance gains are indicated in blue.

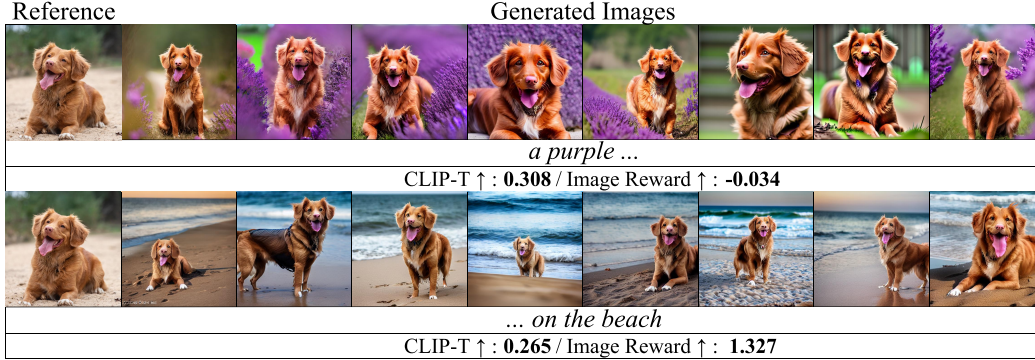


Figure 7: Qualitative examples of T_{CLIP} and ImageReward [50]. Following Instructbooth [7], we measure both T_{CLIP} and ImageReward on 8 displayed images above. Each row illustrates instances where ImageReward provide more accurate evaluations compared to T_{CLIP} . Based on these observations, we additionally evaluate our method using ImageReward.

In main manuscript, we utilize distance-based metrics such as I_{DINO} , I_{CLIP} , and T_{CLIP} to evaluate *identity preservation* and *prompt fidelity*. Specifically, ViT-S/16 DINO [6] and ViT-B/32 CLIP [37] are used to extract the embeddings from the generated and input conditions such as reference images and prompts. Although these metrics show reasonable evaluation results as previous work [5, 42, 34, 46, 53] demonstrated, we often face unexpected results on prompt fidelity evaluation using T_{CLIP} . Fig. 7 illustrates inaccurate evaluation of T_{CLIP} on the generated images. Specifically: (1) In Row 1: even though most images fail to comply with the prompt condition, T_{CLIP} remains relatively high. (2) In Row 2: despite most images successfully adhering to the prompt condition, T_{CLIP} is comparatively low.

To address this issue, recent work [7, 21, 20] suggest to employ a neural network-based evaluation model such as ImageReward [50] that is trained on a large human feedback dataset. We qualitatively validate its robustness as evaluation metric by repeatedly measuring the scores of the generated images. Representative image sets and evaluation results are shown in Fig. 7, where ImageReward demonstrates accuracy, whereas T_{CLIP} as previously discussed tends to relatively inaccurate.

Upon this, we evaluate Layout-and-Retouch using ImageReward to determine how beneficial it is for improving prompt fidelity when plugged into the baseline. Similar to main manuscript, we use ViCo [16] dataset and generate 8 images per object and prompt. Table 5 shows the evaluation on prompt fidelity based on both T_{CLIP} and ImageReward. Layout-and-Retouch greatly improves ImageReward across baselines, demonstrating the strength of our method to generate prompt-aligned images.

B.4 User Study Setup

We conduct user study with aim of evaluating three aspects: (1) *Identity preservation*, (2) *Prompt alignment*, (3) *Diversity of outputs*. As baselines, we compare (1), (2) with three different prior work: MagicFusion [53], FreeU [46], DreamMatcher [34]. Next, we evaluate (3) with DreamMatcher.

The users were given 16 questions to compare identity preservation, 16 questions to compare prompt alignment, and 10 questions to compare diversity of generation. Two *different* sets of question sets were randomly distributed in an attempt to conduct a faithful user study. 48 users answered to 42 questions, resulting in a total of 2,016 responses. Specifically, we design our questions as follows:

- Q1: Please rank the methods (A,B,C,D) for generating an object most similar to the one contained in the following reference image.
- Q2: Please choose the method for generating an image most similar to the given prompt.
- Q3: Please choose the method that generate more diverse images with the given prompt.

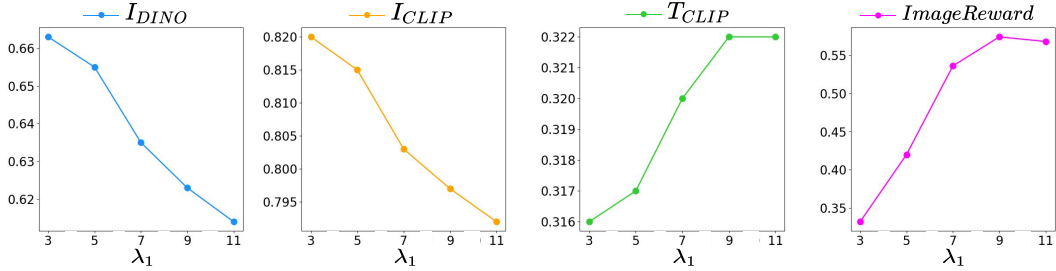


Figure 8: Analysis on the effect of λ_1 of step-blended denoising. Note that the experiments were conducted based on 31 normal ViCo [16] prompts using Dreambooth [42] baseline.

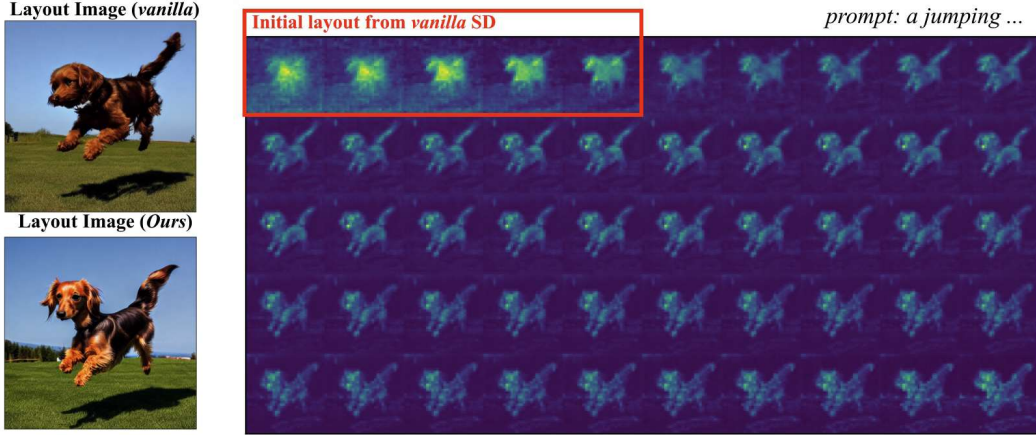


Figure 9: Visualization of the cross-attention map during step-blended denoising. To obtain cross-attention maps, we aggregate the decoder layers of 32 x 32 resolution.

Each question is asked to evaluate (1) *Identity preservation*, (2) *Prompt alignment*, (3) *Diversity of outputs*, respectively. All samples used for the user study were randomly chosen from a pool comprising tens of thousands of images generated from various prompts and object selections using ViCo [16] dataset. For clear understanding, we present an user interface of the user study in Fig. 11 and 12

C Additional Analysis on Layout-and-Retouch

In this section, we analyze our framework Layout-and-Retouch by providing additional experiments with aim of helping to understand the proposed method.

C.1 Analysis on Step-blended Denoising

Hyperparameter sensitivity. Since synthesizing initial layout is critical for Layout-and-Retouch, we empirically analyze the effect of the number of vanilla SD iterations in denoising steps. As shown in Fig. 8, we observe that an early stop of vanilla SD denoising leads to higher identity preservation (I_{DINO} , I_{CLIP}), while simultaneously lowering prompt fidelity (T_{CLIP} , $ImageReward$). On the other hand, as initial layout generation steps increase, identity preservation drops rapidly while the prompt fidelity improves. This demonstrates a trade-off relationship between identity preservation and prompt fidelity as previous work [27] pointed out. Empirically, we determine our optimal λ_1 as five, where identity preservation does not dramatically drop and prompt fidelity is beyond its criterion confirmed in qualitative observation.

Cross-attention map visualization. We visualize a cross-attention (CA) map during step-blended denoising process in Fig. 9. The two images shown in the left side are final images generated using the same seeds, using a solely vanilla denoising and step-blended denoising with $\lambda_1 = 5$. We can observe

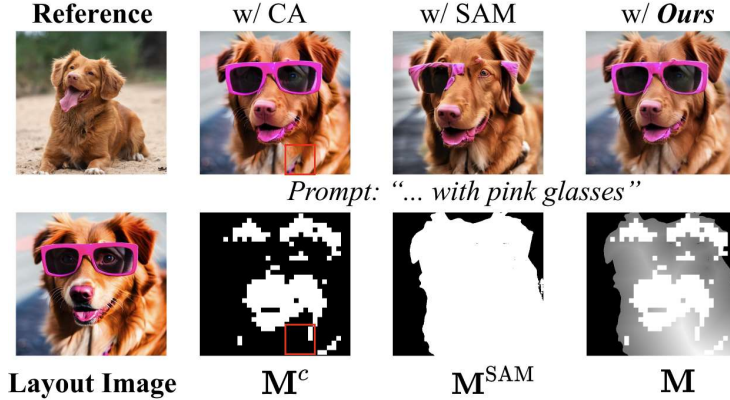


Figure 10: Visualization of each foreground mask and its outputs. We illustrate the masks obtained from different sources and combined mask via adaptive mask blending alongside the generated image for each mask.

that the elements of the image (*e.g.*, dog pose and background) are remarkably similar, suggesting that five denoising iterations suffice to convey a diverse layout from the vanilla model to subsequent steps. Fig. 9 shows detailed visualizations of cross-attention map, which illustrates the alterations in the dog’s form throughout the denoising process. This visualization highlights that modifying only the initial steps with the vanilla model is sufficient for generating diverse and promptly aligned layouts. Subsequent denoising steps employing the pre-trained personalized model further enrich the layout image with ample information about user-specific object

C.2 Qualitative Analysis on Mask Variants

In Fig. 10, we compare our adaptive mask blending method and the mask extracted with SAM [25] and the cross-attention map after thresholding. In the main paper, we argued that utilizing only one of the two masks would result in either noisy region interruption or region misalignment. As seen in Column 2 of Fig. 10, M^c often fail to retrieve the entire foreground object and contains noisy region, resulting in degraded performance in retaining visual details and undesirable artifacts (See red box). On the other hands, Column 2 of Fig. 10 shows that when using only M^{SAM} to define the target region, it often fails to identify important object part, impairing the necessary components of the layout image. To address these issues, we apply adaptive mask blending, successfully overcoming them by finding a balanced mask region and strength.

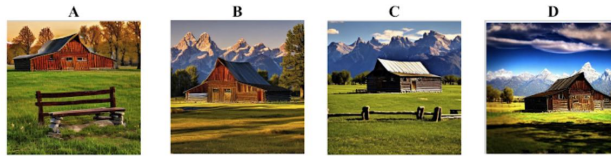
C.3 Additional qualitative results

We additionally report qualitative results of our work as follows:

1. Additional qualitative comparisons with plug-in based baselines across various objects (Fig. 13, 14, and 15).
2. Additional qualitative comparisons by adding the proposed method on baselines (Fig. 16, 17, and 18).
3. Additional comparison with DreamMatcher on image diversity (Fig. 19)

Please rank the methods (A,B,C,D) for generating an object **most similar** to the one contained in the following **reference image**. *

Reference



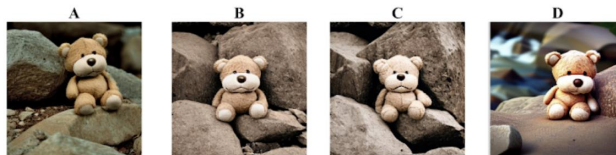
	A	B	C	D
1	<input type="radio"/>	<input type="radio"/>	<input type="radio"/>	<input type="radio"/>
2	<input type="radio"/>	<input type="radio"/>	<input type="radio"/>	<input type="radio"/>
3	<input type="radio"/>	<input type="radio"/>	<input type="radio"/>	<input type="radio"/>
4	<input type="radio"/>	<input type="radio"/>	<input type="radio"/>	<input type="radio"/>

Please choose the method for generating an image **most similar to the given prompt**. *

Reference



Prompt :



	A	B	C	D
1	<input type="radio"/>	<input type="radio"/>	<input type="radio"/>	<input type="radio"/>
2	<input type="radio"/>	<input type="radio"/>	<input type="radio"/>	<input type="radio"/>
3	<input type="radio"/>	<input type="radio"/>	<input type="radio"/>	<input type="radio"/>
4	<input type="radio"/>	<input type="radio"/>	<input type="radio"/>	<input type="radio"/>

Figure 11: **An example of a user study comparing Layout-and-Retouch with prior works:** We compare Identity Preservation and Prompt Alignment with MagicFusion [53], FreeU [46] and Dream-Matcher [34]. For Identity Preservation, we provide a reference image and 4 examples generated by the 4 methods with the same seed. For Prompt Alignment, we additionally provide the prompt that was used to generate the 4 images. The samples were selected randomly from a wide pool for fair comparison.

Please choose the method that **generate more diverse images** with the given *****
prompt

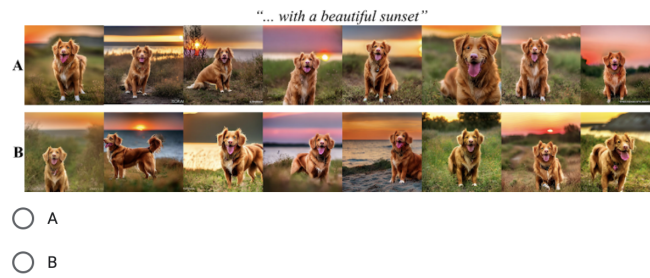


Figure 12: **An example of a user study comparing Layout-and-Retouch with prior works:** We compare Image Diversity with DreamMatcher [34]. We provide the users with a prompt, and the 8 images generated with the same random seeds. The samples were selected randomly from a wide pool for fair comparison.

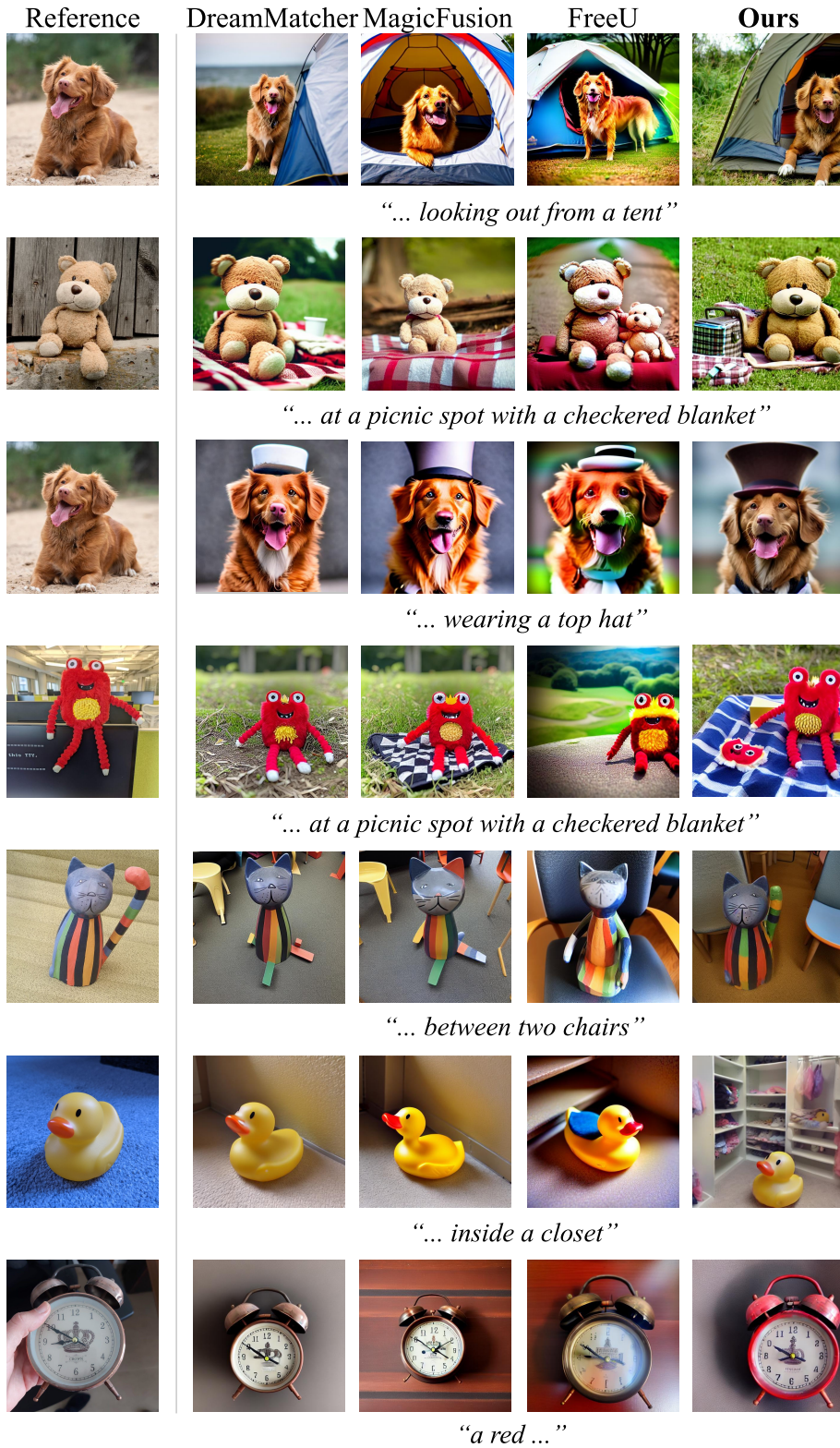


Figure 13: **Qualitative comparison with plug-in based baselines [34, 53, 46]:** We use Dreambooth [42] for all baselines. Note that our method does not produce images with identical structures, as the initial steps of generating layout images rely on vanilla Stable Diffusion [40].

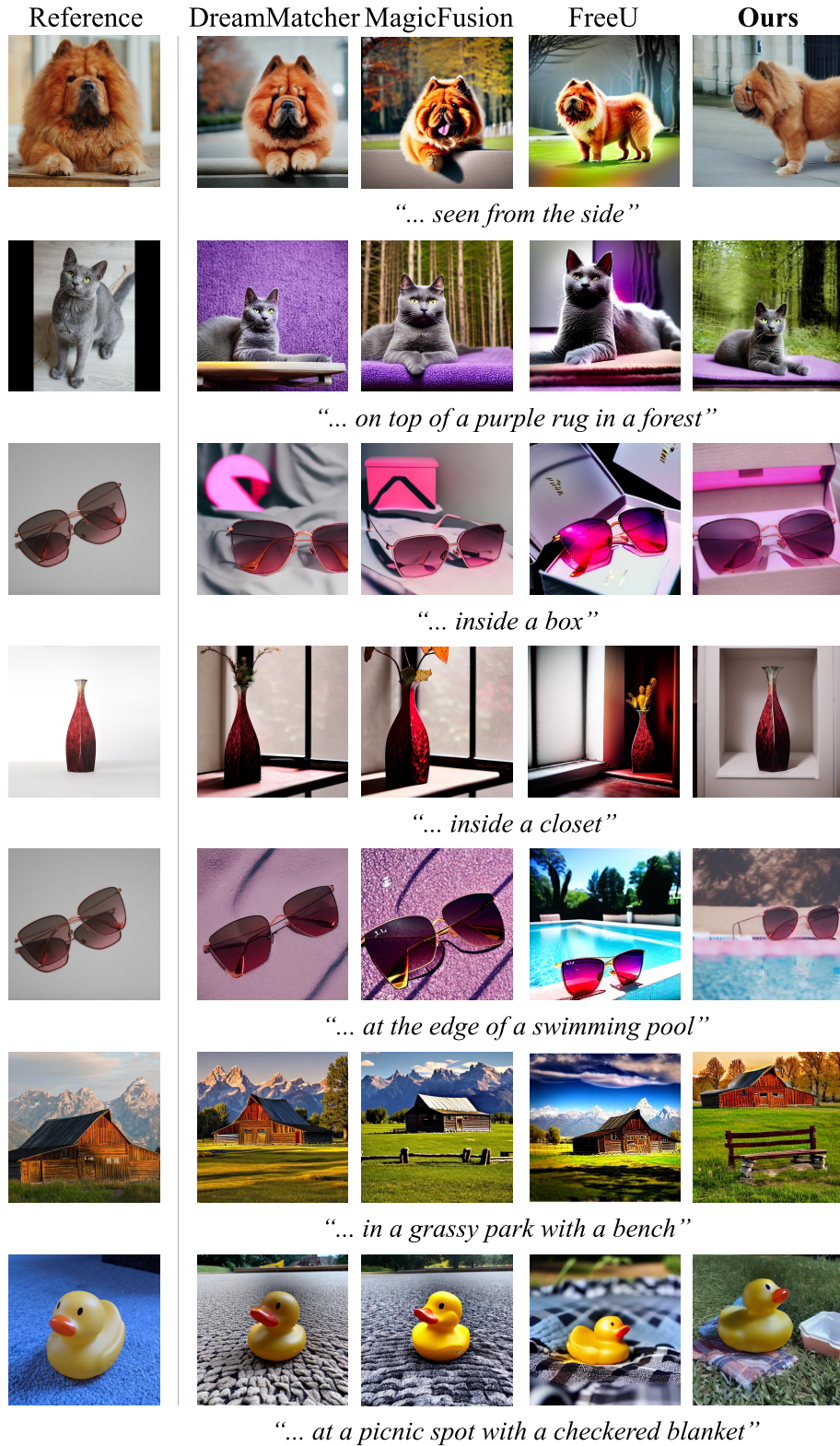


Figure 14: **Qualitative comparison with plug-in based baselines [34, 53, 46]:** We use Dreambooth [42] for all baselines. Note that our method does not produce images with identical structures, as the initial steps of generating layout images rely on vanilla Stable Diffusion [40].

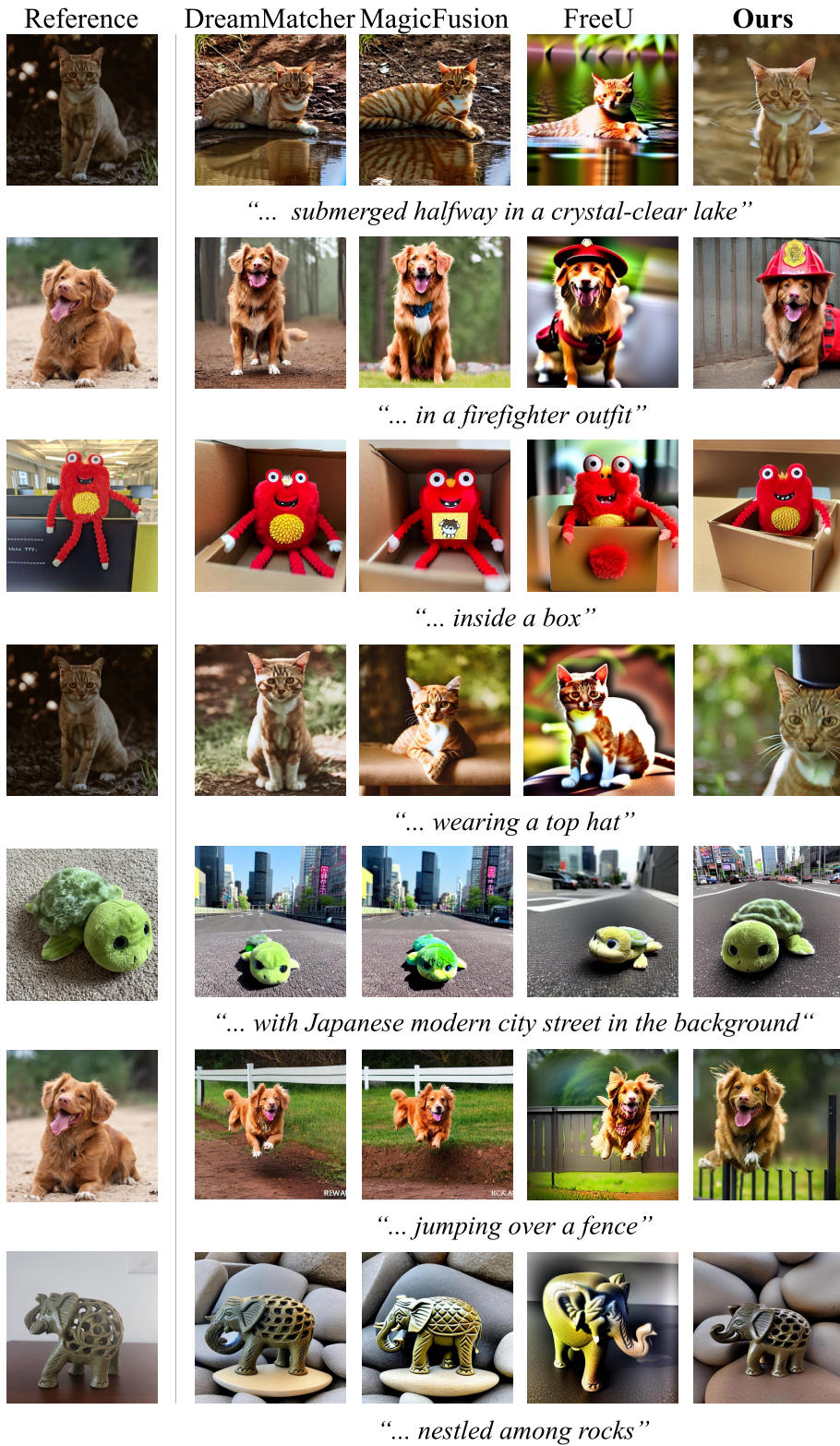


Figure 15: **Qualitative comparison with plug-in based baselines** [34, 53, 46]: We use Dreambooth [42] for all baselines. Note that our method does not produce images with identical structures, as the initial steps of generating layout images rely on vanilla Stable Diffusion [40].

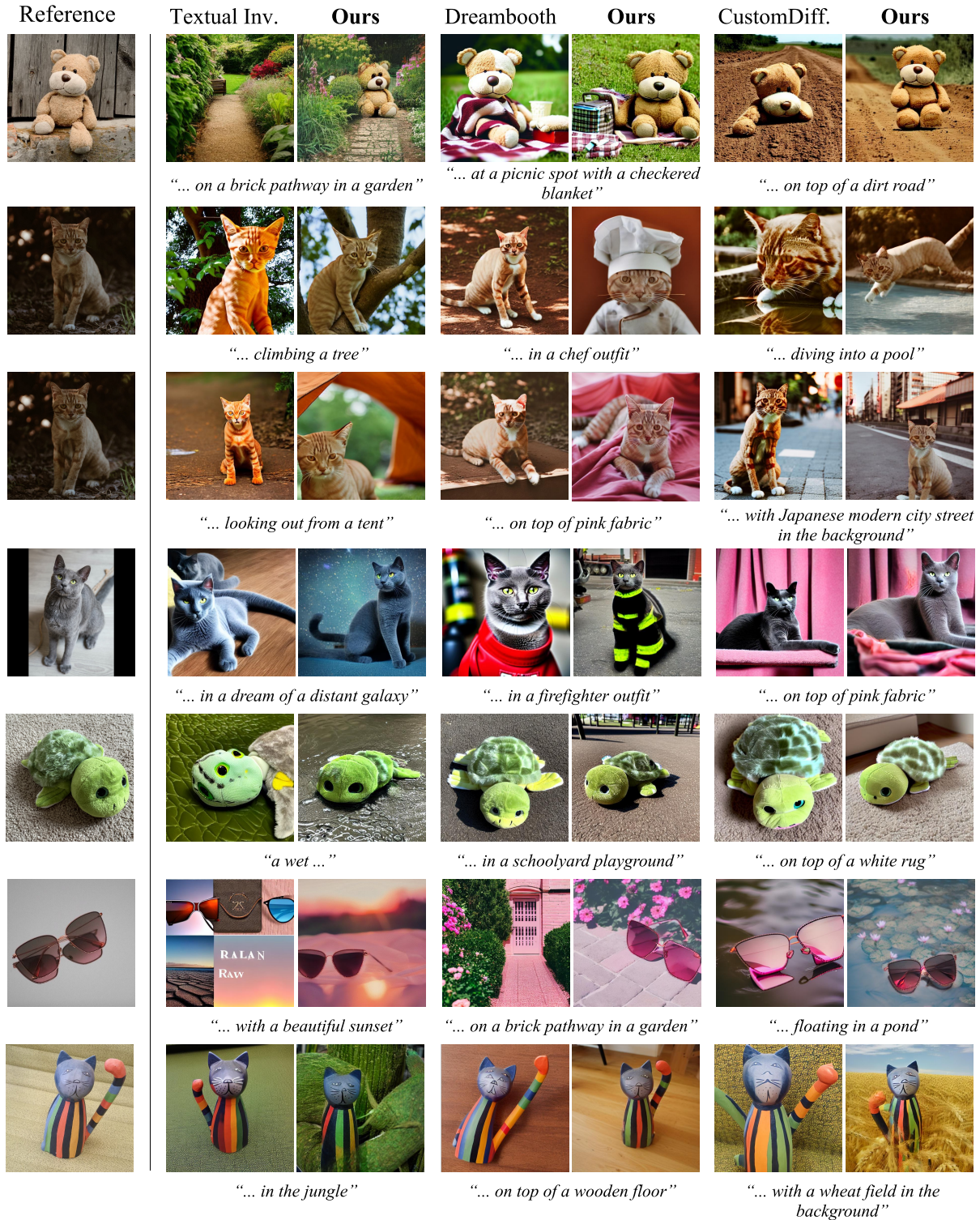


Figure 16: **Qualitative comparison with baselines:** We compare Layout-and-Retouch with the three baseline methods [11, 42, 26] to show the effectiveness of our work. Note that our method does not produce images with identical structures, as the initial steps of generating layout images rely on vanilla Stable Diffusion [40].

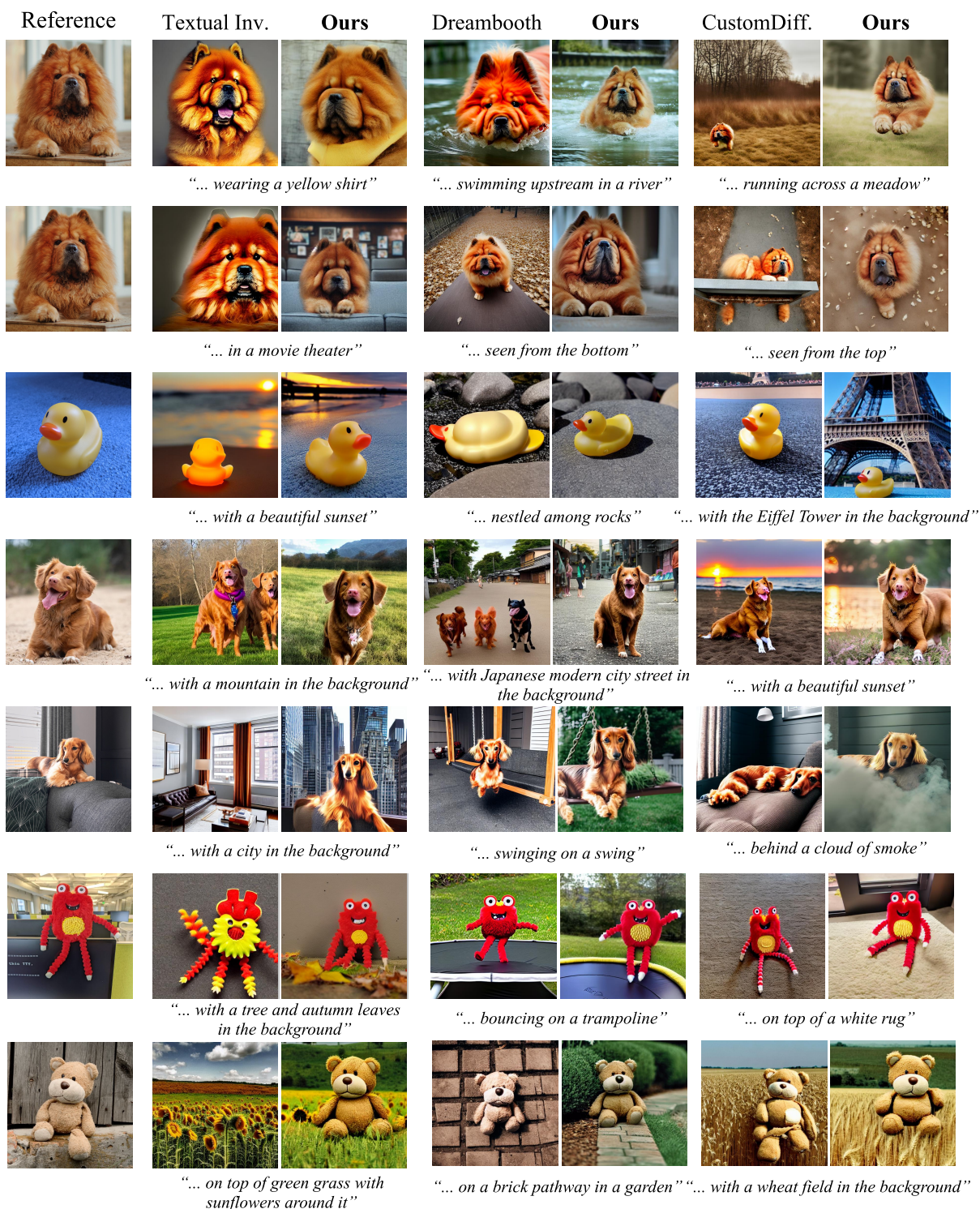


Figure 17: **Qualitative comparison with baselines:** We compare Layout-and-Retouch with the three baseline methods [11, 42, 26] to show the effectiveness of our work. Note that our method does not produce images with identical structures, as the initial steps of generating layout images rely on vanilla Stable Diffusion [40].

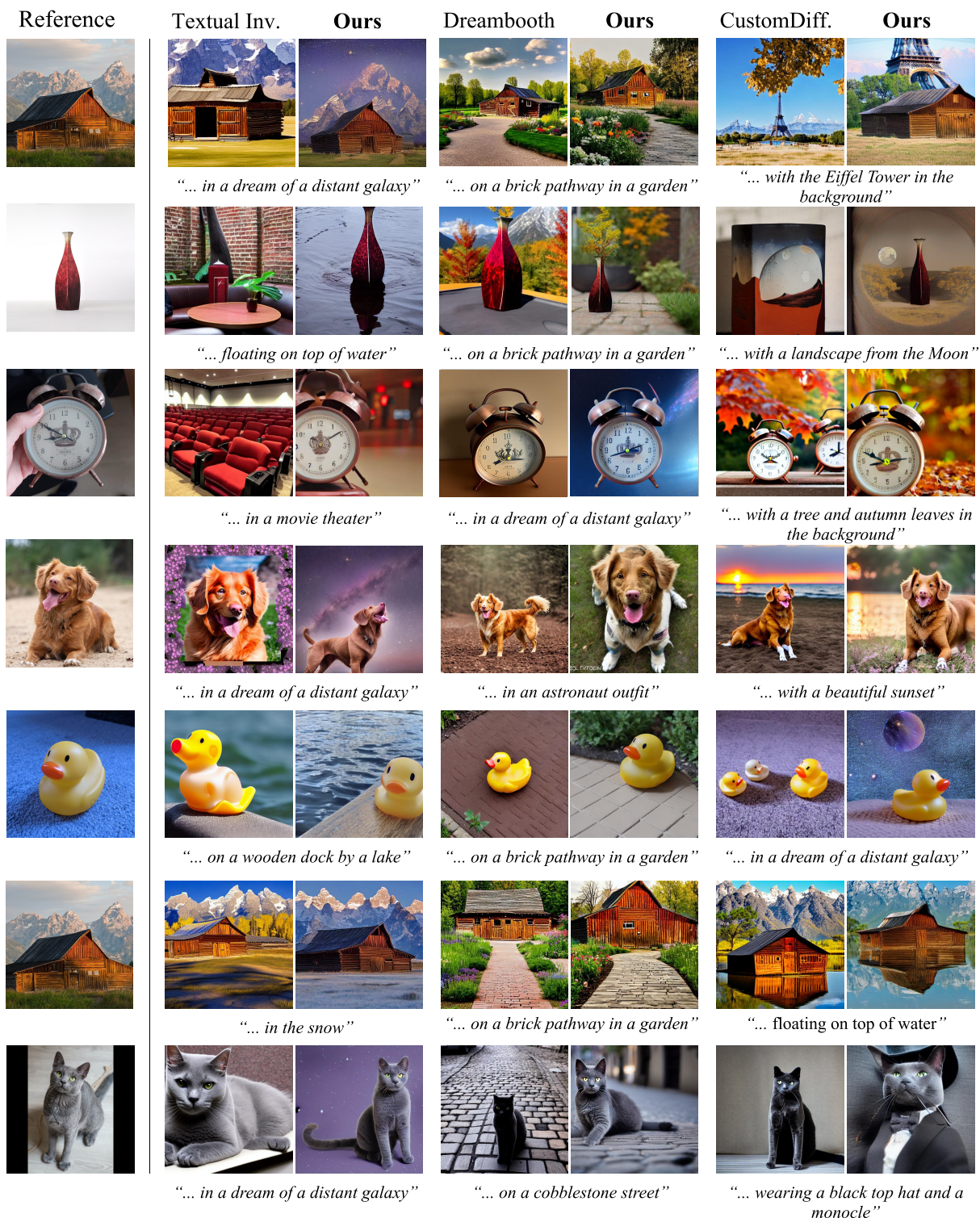


Figure 18: **Qualitative comparison with baselines:** We compare Layout-and-Retouch with the three baseline methods [11, 42, 26] to show the effectiveness of our work. Note that our method does not produce images with identical structures, as the initial steps of generating layout images rely on vanilla Stable Diffusion [40].

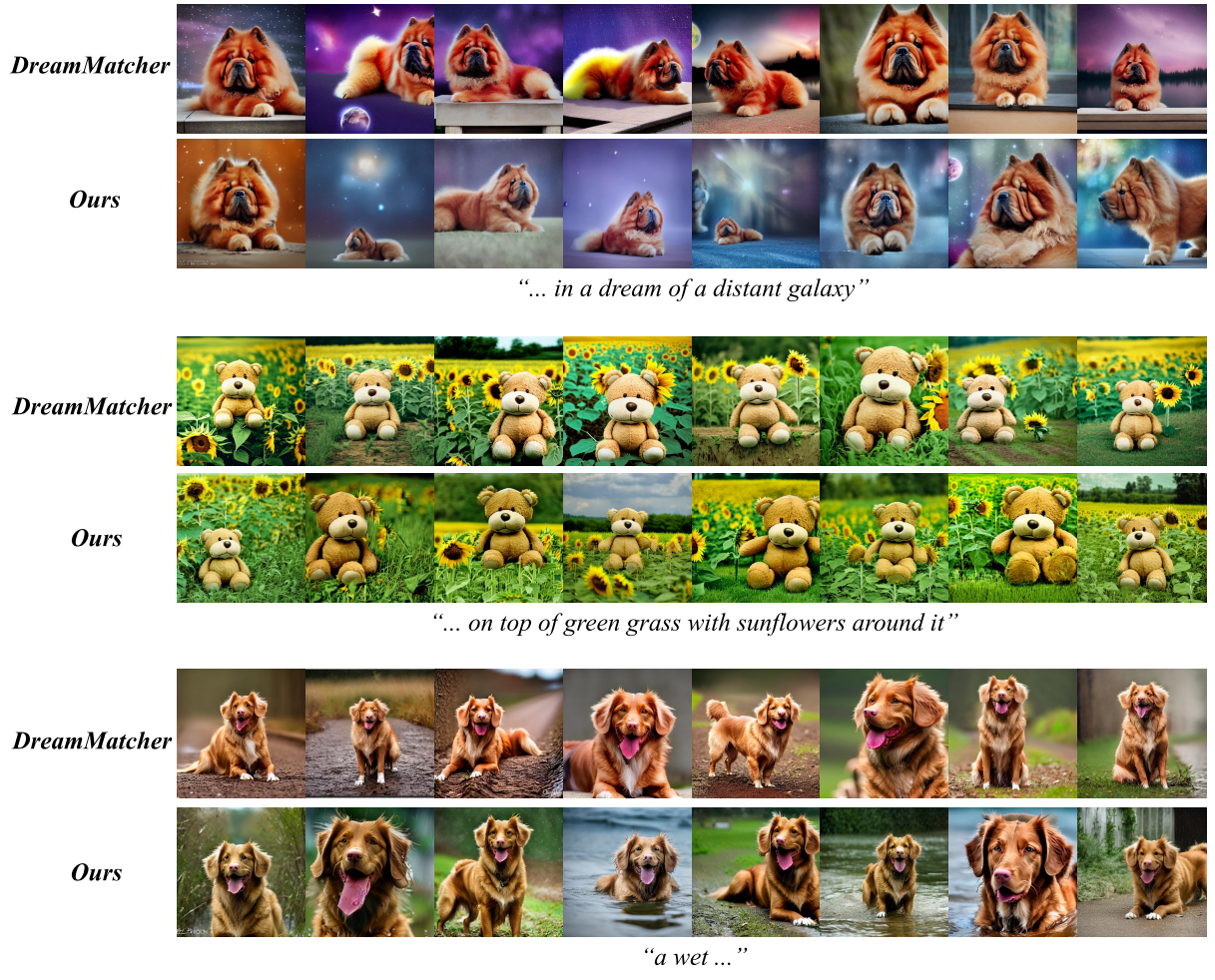


Figure 19: **Diversity comparison against DreamMatcher [34]:** We present the generated images of Layout-and-Retouch and DreamMatcher, to highlight the capacity of the proposed approach in producing diverse images.